GeoConvention 2015
GEOSCIENCE
new horizons
Telus Convention Centre • 4-8 May 2015 • Calgary, AB Canada

Extending LMR for anisotropic unconventional reservoirs

Marco A. Perez
Apache Canada Ltd

Summary

It has become increasingly advantageous to characterize rock in unconventional reservoirs within an anisotropic framework. Previous work has shown that anisotropy is linked to the presence of oriented fractures, stress and kerogen amongst other reservoir properties. These properties all impact hydraulic stimulation efforts and play an important role in the ability to produce low permeability reservoirs. Logging wellbores, vertical or horizontal, does not give a complete understanding of anisotropic nature of the reservoir as it only measures formation slowness in one direction. However, the geometries associated with modern seismic acquisition are able to more completely determine anisotropic parameters from reflection and traveltime data recorded over numerous propagation directions.

To analyze and interpret the seismically derived anisotropic attributes, the LMR crossplot is extended to consider anisotropic components of the stiffness tensor. The anisotropic version of LMR attributes is associated to rock properties beyond lithology as it is now related to fabric and oriented crack geometry. Vertical transverse isotropy is investigated using published rock physics models. A method is presented that illustrates how to interpret the expanded attributes and how seismic attributes can help in understanding the elastic properties of reservoir rock with respect to potential completion efforts ramifications.

Introduction

The Lambda-Mu-Rho (LMR) attritbutes were introduced by Goodway et al (1997) as a way to distinguish varying lithology and fluid content from seismic attributes. It introduced a different perspective on elastic rock properties distinct from the conventional compressional (P) velocity or impedance and shear (S) velocity or impedance (or the ratio) attribute crossplots. To illustrate the point, consider the elastic stiffness tensor represented as a matrix using the Voigt notation,

$$C = \begin{bmatrix} c_{11} & c_{12} & c_{13} & & & \\ c_{21} & c_{22} & c_{23} & & & \\ c_{31} & c_{32} & c_{33} & & & \\ & & & c_{44} & & \\ & & & & c_{55} & \\ & & & & & c_{66} \end{bmatrix}. \tag{1}$$

The upper diagonal components represent the P-wave propagation while the lower diagonal components are the shear components. The c_{11} component is represented in terms of Lame parameters is

$$c_{11} = \lambda + 2\mu \tag{2}$$

which is the P-wave modulus. The lower half of the diagonal is expressed as

$$c_{44} = \mu \,. \tag{3}$$

The off diagonal component in isotropic media is simply

$$c_{12} = c_{13} = c_{23} = \lambda \tag{4}$$

where λ is the modulus relating normal stress to a perpendicular strain.

The difference between a Vp Vs crossplot and an LMR crossplot is simply different components of the elastic stiffness tensor: on diagonal versus off diagonal stiffness components. The variation in c_{11} and c_{13} in the lithologies of interest will determine which space is more suitable for interpretation. It is noted that computing c13 in the special case of isotropic media is given by

$$c_{13} = c_{11} - 2c_{44} \,. \tag{5}$$

For anisotropic media, computing c_{13} is not as straightforward. Given the geometries present within logging programs, only certain parts of the elastic stiffness tensor can be measured. For example, a vertical wellbore measuring compressional and shear traveltimes populates the c_{33}, c_{44} and c_{55} components of the stiffness tensor shown in figure 1.

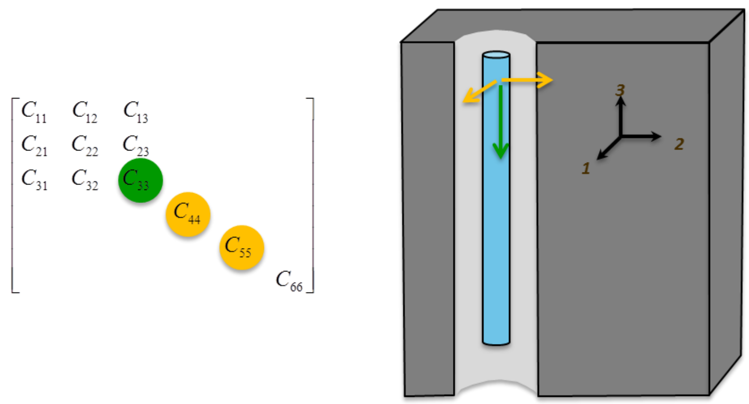

Figure 1. Schematic showing vertical borehole and measurable components of stiffness tensor.

The green and yellow arrows in figure 1 show particle motion for a vertical propagation corresponding to P and S waves respectively. Similarly, in a horizontal well drilled in the x_1 direction, the c_{11}, c_{55} and c_{66} are measured. For vertical transverse isotropy, the 5 independent elastic stiffness components are shown below as well as an equivalent form in terms of Lame parameters (adapted from Goodway, 2001)

$$c_{VTI} = \begin{bmatrix} c_{11} & c_{11}-2c_{66} & c_{13} & & & \\ c_{11}-2c_{66} & c_{11} & c_{13} & & & \\ c_{13} & c_{13} & c_{33} & & & \\ & & & c_{44} & & \\ & & & & c_{44} & \\ & & & & & c_{66} \end{bmatrix} = \begin{bmatrix} \lambda_H+2\mu_H & \lambda_H & \lambda_T & & & \\ \lambda_H & \lambda_H+2\mu_H & \lambda_T & & & \\ \lambda_T & \lambda_T & \lambda_V+2\mu_V & & & \\ & & & \mu_V & & \\ & & & & \mu_V & \\ & & & & & \mu_H \end{bmatrix} \tag{6}$$

In a vertical borehole, the measured traveltimes fail to provide any information for c_{11}, c_{12}, c_{66} and c_{13} (any of the horizontal and transverse components. To fill in the information gap, seismic data and a rock physics model is used to help constrain and ultimately interpret attributes derived from seismic data.

Method

The effective field model (EFM) is used to characterize VTI rocks that are either intrinsically anisotropic, contains some anisotropic components or has oriented inclusions (pores and/or cracks). Rock phsyics models are constructed that show the interrelationship between the components of the elastic stiffness tensor and anisotropic geometry using the method presented by Sevostianov et al (2005) with seismic application examples shown by Sayers (2013),.

The LMR crossplot space is expanded to visualize the anisotropic tensor. It considers not only the c_{13} and c_{44} components but also the other off diagonal and shear components, c_{12} and c_{66}. Conventional LMR is but a subset of the potential crossplot space. Extending the crossplot space demonstrates how the elastic parameters vary with respect to anisotropic geometry (VTI versus HTI for example) and expected seismic response. An appropriate crossplot space now includes crossplotting the two independent shear components (c_{44} and c_{66} in VTI media) against the two independent off diagonal terms (c_{12} and c_{13} in VTI media). Figure 2a shows the log data in an isotropic LMR crossplot while figure 2b shows the same log data transformed using $\varepsilon = 0.15$ and $\delta = \gamma = 0.1$ with anisotropic rock physics trends. Well data in both figures is color coded by quartz volume. The geometry of the anisotropic rock, fit to log data with seismic estimates of ε and δ, helps interpret the elastic properties.

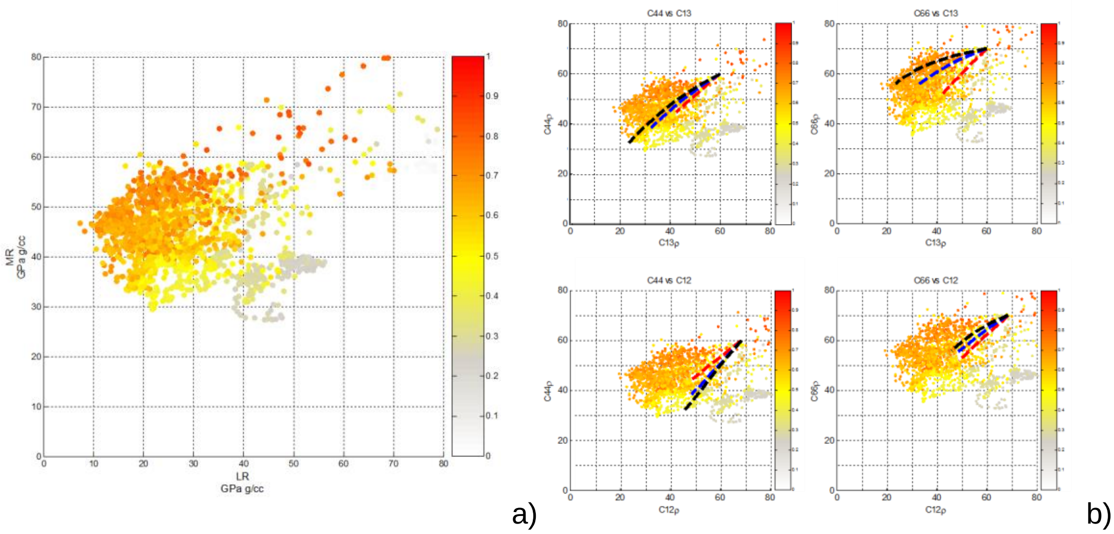

Figure 2. Left) Isotropic LMR crossplot Right) c13,c12, c44 and c66 crossplot with anisotropic rock rock physics trends with varying pore aspect ratio (α). Red $\alpha = 1$, Blue $\alpha = 5$, Black $\alpha = 10$.

As Goodway (2001) has noted, δ represents the off diagonal component of the elastic tensor, obtainainable from surface seismic data. From this perspective, the extended LMR crossplot provides insight to seisimically derived estimates of anisotropy, in particular δ. As shown by Sayers (1995), to first order δ is a function of c_{13}, through

$$\chi = \frac{(c_{13} + 2c_{44} - c_{33})}{c_{33}} \tag{7}$$

with

$$\delta = \chi + \frac{\chi^2}{2(1 - c_{44}/c_{33})} \tag{8}$$

Since $c_{44} = Vp^2$ and $c_{33} = Vs^2$, c_{13} can be computed with a seismic estimate of δ. Note that when $c_{13} + 2c_{44} < c_{33}$ negative δ occur. In such cases, the c_{44} c_{13} crossplot should display a skew towards the origin while a positive δ will move away. Comparing measured variations in anisotropy with EFM anisotropic models allows for interpretation of reservoir fabric.

Applications

An integrated model can be constructed to account for anisotropy present in unconventional reservoirs using well data, estimated values of ε and δ, and rock physics models. Below are some applications utilizing anisotropic parameters.

Stress Profiling

Stress profiling has been discussed by Vernik and Milovac (2011) and Sayers (2013) showing the impact and increased stress as a function of λ_T (c_{13}). The stress perturbations equations for VTI media are given by Sayers (2013) where

$$\sigma_1 = \alpha p + \frac{c_{13}}{c_{33}}(\sigma_3 - \alpha_3 p) + \left(c_{11} - \frac{c_{13}^2}{c_{33}}\right)^2 \varepsilon_1 + \left(c_{12} - \frac{c_{13}^2}{c_{33}}\right)\varepsilon_2 \tag{9}$$

$$\sigma_2 = \alpha p + \frac{c_{13}}{c_{33}}(\sigma_3 - \alpha_3 p) + \left(c_{12} - \frac{c_{13}^2}{c_{33}}\right)^2 \varepsilon_1 + \left(c_{11} - \frac{c_{13}^2}{c_{33}}\right)\varepsilon_2 \,.$$

For uniaxial strain ($\varepsilon_1 = \varepsilon_2 = 0$) the c_{13}/c_{33} ratio determines stress perturbation. The c_{13} component can be measured seismically through δ derived either from fourth other moveout analysis or amplitude variation with offset.

Anisotropic Rock Strength

Aside from estimating stress perturbations, another possible application is determining strength anisotropy (Jaeger et al, 2007). Given the presence of elastic anisotropy it is likely that strength anisotropy is also present.

The condition for shear failure is described mathematically as

$$\tau = \frac{1 - \sin\phi}{2\cos\phi} UCS + \tan\phi \tag{10}$$

where UCS is the unconfined compressive strength and ϕ is the angle of internal friction. With the strong correlation between Young's modulus (E) and UCS, elastic anisotropy would indicate strength anisotropy.

For VTI media there are two measurable E, horizontal (E_h) and vertical (E_v) defined as

$$E_h = \frac{(c_{11} - c_{12})}{c_{11}c_{33} - c_{13}^2}\left(c_{33}(c_{11} + c_{12}) - 2c_{13}^2\right) \tag{11}$$

$$E_v = \frac{c_{33}(c_{11} + c_{12}) - 2c_{13}^2}{c_{11} + c_{12}} \tag{12}$$

Figure below shows how variations in c_{13} only, change δ and vertical and horizontal Young's modulus.

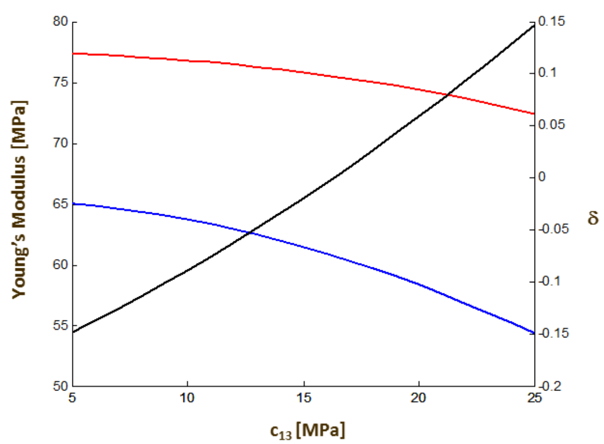

Figure 3. Vertical (blue) and horizontal (red) Youngs modulus and δ (black) as a function of c_{13}

Associating the variations in δ with the rock physics models with respect to expected mineralogy and porosity variations can help in assessing the significance of the anisotropic parameters, whether it be associated with intrinisic matrix anisotropy or preferentially aligned cracks. The difference between intrinsic and oriented inclusions will impact completions perfomance. The in-situ stress state, its orientation with respect to the symmetry axis of the anisotropic rock and rock strength anisotropy will result in different types of failure. Taking into consideration the variable rock strength and stress state can help in predicting completion efficacy and accelerate optimization of future programs.

Conclusions

The LMR attritbutes are a subset of the elastic stiffness tensor which can be extended to consider different anisotropic parameters. Because LMR focuses on the off diagonal component fo the tensor, it inherently represents the important parameter in determining stress perturbations. It also can show potential variation in rock strength by variation in the shear modulus. Using published rock physics models can help in giving phsyical significance to the observed anisotropy leading to better reservoir characterization of unconventional plays. As always, it is important to calibrate models and seismic estimates to well and core data when available.

References

Goodway, B., 2001, AVO and Lame' constants for rock parameterization and fluid detection: Recorder, **26** , no. 6, 39-60.
Goodway, W., Chen, T., and Downton, J., 1997, Improved AVO fluid detection and lithology discrimination using Lamé petrophysical parameters; "Lambda-Rho", "Mu-Rho", & "Lambda/Mu fluid stack", from P and S inversions: 67 Annual Internat. Mtg., Soc. Expl. Geophys., Expanded Abstracts, 183-186.

Sayers, 2013, The effect of kerogen on the elastic anisotropy of organic-rich shales: Geophysics, 78, 65-74.

Sayers, 2005, Seismic anisotropy of shales: Geophysical Prospecting, 53, 667-676.

Sevostianov, I., N. Yilmaz, V. Kushch, and V. Levin, 2005, Effective elastic properties of matrix composites with transversely-isotropic phases: International Journal of Solids and Structures, 42, 455–476.

Sayers, 1995. Simplified anisotropy parameters for transversely isotropic sedimentary rocks, Geophysics, 60,1933-1935

Vernik L., and Milovac, J., 2011, Rock physics of organic shales: The Leading Edge, March, 318-323.

Hashemi, M., Ghazvinian, A., & Taghichian, A. (2009, January). Exact Satisfaction of Uniaxial Tensile And Compressive Strengths of Rock In a New Failure Criterion Considering Brittle-Ductile Transition As an Initial Boundary Condition. In Proceedings of the 2009 International Symposium on Rock Mechanics:" Rock Characterisation, Modelling and Engineering Design Methods.

Jaeger, J.C., Cook, N.G.W., Zimmerman, R.W.: Fundamentals of Rock Mechanics. Blackwell Publishing, Malden (2007)